Synthesis and Photoresponsive Behaviors of Well-Defined Azobenzene-Containing Polymers via RAFT Polymerization

Yuanyuan Zhang,[†] Zhenping Cheng,[†] Xinrong Chen,[‡] Wei Zhang,[†] Jianhong Wu,[‡] Jian Zhu,[†] and Xiulin Zhu*,[†]

Key Laboratory of Organic Synthesis of Jiangsu Province, School of Chemistry and Chemical Engineering, Suzhou University, Suzhou 215006, China, and Institute of Information Optical Engineering, Suzhou University, Suzhou 215006, China

Received January 29, 2007; Revised Manuscript Received April 30, 2007

ABSTRACT: The well-defined photoresponsive polymethacrylate containing azo chromophore, poly{1′-octyloxy-4′-(6-methacryloxy)hexyloxy-5′-phenylmethaneone-(2-phenyl)azobenzene (AHMA)} (PAHMA), was prepared via reversible addition−fragmentation chain transfer (RAFT) polymerization in anisole solution using 2-cyanoprop-2-yl 1-dithionaphthalate (CPDN) as the RAFT agent and 2,2′-azobis(isobutyronitrile) (AIBN) as an initiator. The kinetic plots of polymerization were first-order and the molecular weights ($M_{n(GPC)}$s) of the homopolymer (PAHMA) with relatively low polydispersity index values (PDIs ≤ 1.37) increased with monomer conversions throughout the polymerization processes. Furthermore, the kinetic plots of chain extension with both methyl methacrylate (MMA) and styrene (St) using the obtained PAHMA as a macro-RAFT agent were also first-order. The $M_{n(GPC)}$s of the diblock copolymers, PAHMA-*b*-PMMA and PAHMA-*b*-PS, increased with the respective monomer conversions. These results indicated that most of the PAHMA chains were still "living". The structure and properties of the polymers were characterized by ^{1}H NMR, GPC, and UV−vis spectra. The photoisomerization of the polymer was examined. On irradiation with a linearly polarized Kr^+ laser beam, the birefringence was induced in the polymer films to the level of 0.075. With illumination of linearly polarized Kr^+ laser beam at modest intensities (120 mW/cm^2), significant surface relief gratings (SRGs) formed on the polymer films were observed.

Introduction

In recent years, azobenzene-containing polymers (azo polymers) have attracted considerable attention because of their unique reversible photoisomerization between the trans-to-cis isomers of the chromophore, where large changes occur in its size, shape, and polarity.[1,2] Azo polymers have potential applications in many fields, which include optical data storage,[3,4] liquid crystal displays,[5] and holographic surface relief gratings.[6,7] For reversible optical storage and correlative applications, polarized light has been used to induce reorientation of the azobenzene groups through repeated trans−cis photoisomerization and subsequent cis−trans relaxation of azobenzene groups.[8,9] This anisotropic molecular reorientation induces both birefringence and dichroism properties changing in the materials.[10−12] Furthermore, the surface relief gratings (SRGs) can be formed directly on azo polymer films by exposure of the polymer to the interfering laser beams.[6,7,11,13] The SRGs are stable below the glass transition temperatures (T_gs) of the polymers and can be removed by heating samples to their T_gs or erased even below their T_gs.[11,14,15] Several models were proposed for the mechanism of the surface grating formation, but these are still under discussion.[16−18] In all cases, the photochemical trans−cis−trans isomerization cycles of the azo chromophores seemed to play a key role in the process of large-scale polymer chain migration that induces the gratings either on the surface or in the bulk.[2,19]

Most side-chain azo polymers were prepared by common free radical polymerization with uncontrolled molecular weights and relatively large polydispersity index values. In order to conquer these drawbacks, Solaro et al.[20] reported that the anionic copolymerization of 4-vinylazobenzene and styrene using butyllithium as an initiator resulted in low monomer conversion and low molecular weight. Aoshima et al.[21] reported the synthesis of copolymers with various types of azobenzene side groups via living cationic polymerization and studied the photoresponsive behavior of the obtained copolymers. However, the conditions of anionic and cationic polymerization are stringent, such as the need for highly purified reagents and low reaction temperature. Fortunately, living free radical polymerization (LFRP), such as atom transfer radical polymerization (ATRP),[22−24] and reversible addition−fragmentation chain transfer (RAFT)[25−28] polymerization in particular have become the most popular methods with less stringent experimental conditions. Up to now, ATRP or a combination of ATRP method has been successfully used to synthesize azo polymers with well-defined structures.[29−34] Zhao et al.[31,32] reported the preparation of a series of liquid-crystalline diblock or triblock copolymers with an azobenzene moiety in the side chain. As the other powerful LFRP methods, the RAFT technique has been widely used to synthesize functional polymers because of its high degree of compatibility with a wide range of functional monomers and good tolerance of water and oxygen in the systems.[35] However, to the best of our knowledge, no investigation has been reported on the synthesis of azo polymers via the RAFT polymerization method. The use of block copolymers is a simple way to obtain materials with quite different properties by adjusting amounts of opposing monomers.[36] As one of the most versatile techniques, RAFT polymerization has been used widely to prepare block copolymers.[37−39]

In recent years, most of the researches were performed on donor−acceptor substituted azobenzene, typically amino−nitro substituted,[11,40−42] but less attention was paid to no donor−acceptor substituents azobenzene, as its thermal cis−trans isomerization is relatively low and the maximum absorbance

* Corresponding author: Fax 86-512-65112796; e-mail xlzhu@suda.edu.cn.
[†] School of Chemistry and Chemical Engineering.
[‡] Institute of Information Optical Engineering.

10.1021/ma070257i CCC: $37.00
Published on Web 06/16/2007

Scheme 1. Synthetic Routes of AHMA and PAHMA Homopolymer[a]

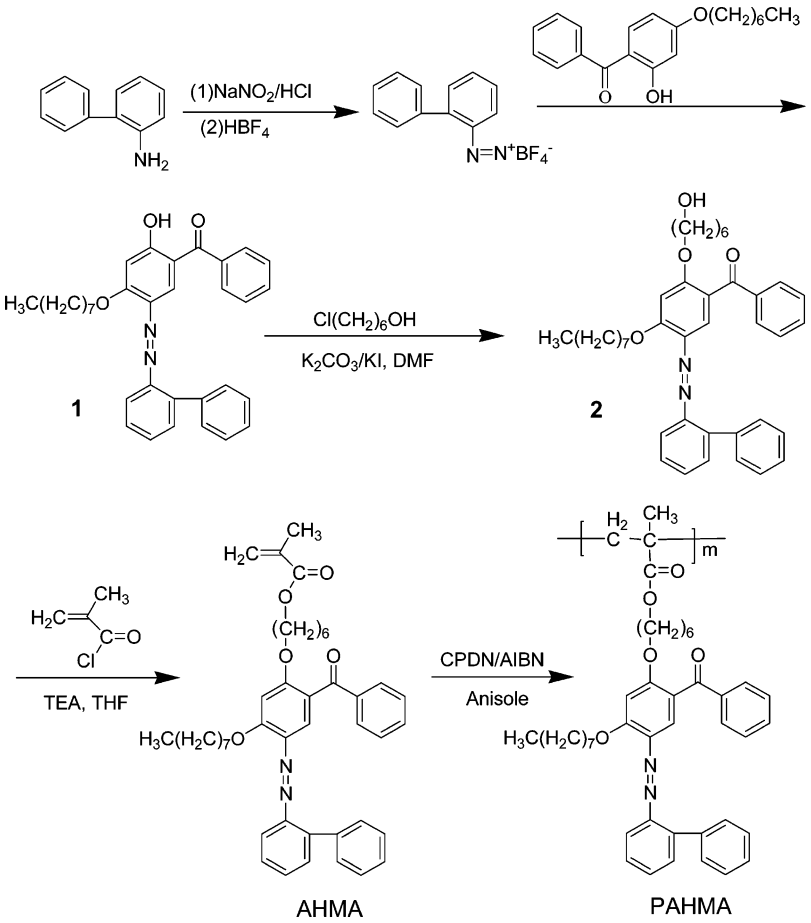

[a] AHMA = 1′-octyloxy-4′-(6-methacryloxy)hexyloxy-5′-phenylmethaneone-(2-phenyl)azobenzene; PAHMA = poly{1′-octyloxy-4′-(6-methacryloxy)hexyloxy-5′-phenylmethaneone-(2-phenyl)azobenzene}; DMF = dimethylformamide; TEA = triethylamine; THF = tetrahydrofuran; CPDN = 2-cyanoprop-2-yl-1-dithionaphthalate; AIBN = 2,2′-azobis(isobutyronitrile).

shift toward higher energy (shorter wavelength) for the trans isomer. Here, a new azo monomer 1′-octyloxy-4′-(6-methacryloxy)hexyloxy-5′-phenylmethaneone-(2-phenyl) azobenzene (AHMA; Scheme 1) without donor−acceptor substituent was designed. The AHMA homopolymer (PAHMA) and diblock copolymers (PAHMA-*b*-PMMA and PAHMA-*b*-PS) were synthesized with well-controlled molecular weights and low polydispersity index values via RAFT polymerization. The photoisomeric behavior and the birefringence of the azo polymer were measured, and the SRGs were also prepared using the azo polymer.

Experimental Section

Characterization. The measured number-average molecular weight ($M_{n(GPC)}$s) and polydispersity index values (PDIs) of the polymers were determined with a Waters 1515 gel permeation chromatograph (GPC) equipped with a refractive index detector, with HR1, HR3, and HR4 columns with a molecular weight range of 100−500 000 and calibrated with poly(methyl methacrylate) (PMMA) standard samples. Tetrahydrofuran (THF) was used as the eluent at a flow rate of 1.0 mL/min at 30 °C. ^{1}H nuclear magnetic resonance (NMR) spectra were recorded on Inova 400 MHz nuclear magnetic resonance instrument with dimethyl sulfoxide (DMSO-d_6) or chloroform ($CDCl_3$) as a solvent and tetramethylsilane as the internal standard. The UV−vis absorption spectra of the polymers in chloroform solutions were determined on a Shimadzu-RF540 spectrophotometer.

The birefringence measurement was produced with a pump Kr^+ laser beam (413.1 nm, 20 mW/cm^2) polarized at 45° with respect to the probe beam polarization. The experimental setup is shown in Figure 2. The sample was placed between two crossed polarizers. The transmitted probe beam (650 nm diode laser) was detected by a photoelectric cell and connected through an amplifier to a computer. The other experimental setup for surface relief gratings (SRGs) fabrication was similar to other groups reported before.[6] A linearly polarized Kr^+ laser beam (413.1 nm, 120 mW/cm^2) was used as the light source. SRGs were optically inscribed on the polymer films with p-polarized interfering laser beams. The surface images of the surface relief gratings were probed using atomic force microscopy (AFM) (NT-MDT SOLVER P47-PRO). The diffraction efficiency of the gratings was monitored by measuring the first-order diffracted beam intensity of an unpolarized low-power diode laser beam (650 nm) in transmission mode.

Materials. Unless otherwise specified, all chemicals (99+%) were purchased from Shanghai Chemical Reagent Co. Ltd. Styrene (St, 99%) and methyl methacrylate (MMA, 99%) were washed with a 5% sodium hydroxide aqueous solution and then with deionized water until neutralization, after being dried with anhydrous magnesium sulfate overnight, distillated over CaH_2 under vacuum, and stored at −18 °C. 2,2′-Azobis(isobutyronitrile) (AIBN, 97%) was recrystallized from ethanol twice, dried at room temperature in vacuum, and stored at −18 °C. Anisole (analytical reagent) and chloroform (analytical reagent) were used after distillation. 2-Aminobiphenyl (Fluka, 98%), 2-hydroxy-4-(octyloxy)benzophenone (Acros, 98%), and 1-chloro-6-hydroxyhexane (Acros, 95%) were used as received. 2-Cyanoprop-2-yl-1-dithionaphthalate (CPDN, Chart 1) was synthesized according to the method described previously,[43] and the purity of it is above 95%.

Monomer Synthesis. 1′-Octyloxy-4′-hydroxy-5′-phenylmethaneone-(2-phenyl)azobenzene (1). 2-Aminobiphenyl (5.1 g, 30 mmol) was dissolved in hydrochloric acid (15 mL) and deionized

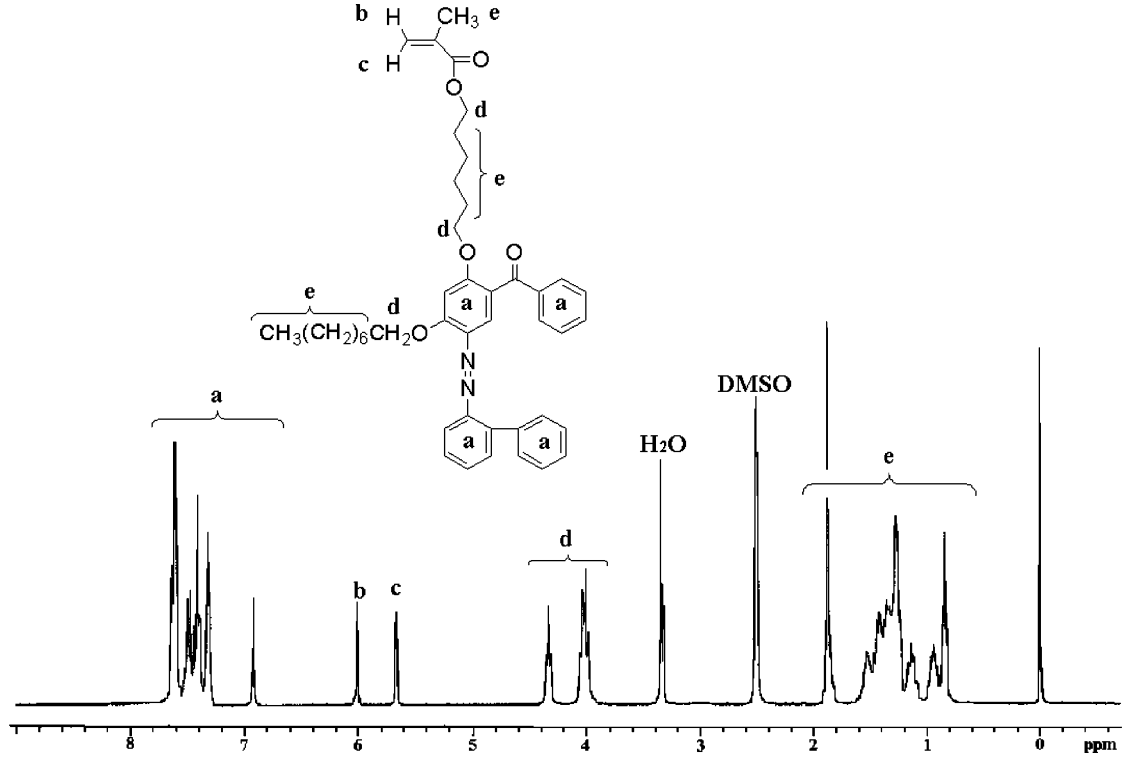

Figure 1. ^{1}H NMR spectrum of the monomer AHMA in DMSO-d_6. AHMA = 1′-octyloxy-4′-(6-methacryloxy)hexyloxy-5′-phenylmethaneone-(2-phenyl)azobenzene; AHMA was synthesized as follows: By coupling reaction of 2-hydroxy-4-(octyloxy)benzophenone with diazotized 2-aminobiphenyl, the above product was reacted with 1-chloro-6-hydroxyhexane, and then the obtained compound was reacted with methacryloyl chloride to obtain the ultimate product AHMA.

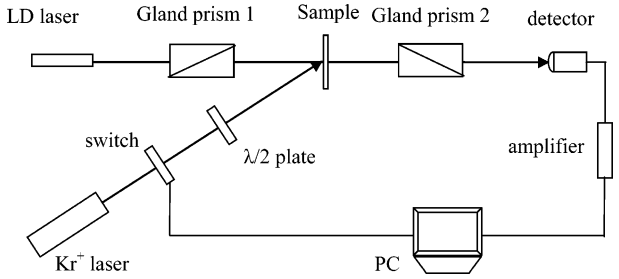

Figure 2. Setup for producing and detecting the birefringence effect of the sample.

Chart 1. Chemical Structures of CPDN and AHMA[a]

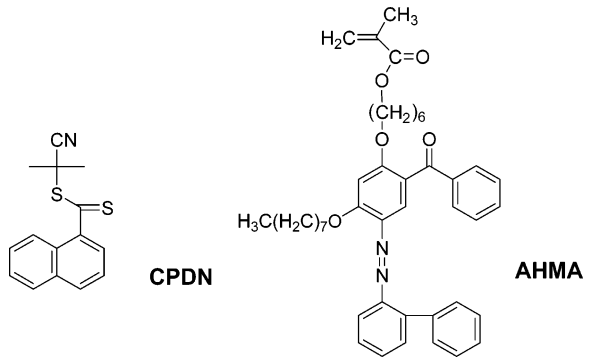

[a] CPDN = 2-cyanoprop-2-yl-1-dithionaphthalate; AHMA = 1′-octyloxy-4'-(6-methacryloxy)hexyloxy-5′-phenylmethaneone-(2-phenyl)azobenzene.

water (80 mL). The mixture was stirred in an ice bath, and then sodium nitrite (3.0 g) in 30 mL of deionized water was added dropwise. The mixture reacted at 0−5 °C for 30 min and was filtered. Then, 30 mL of fluoroboric acid was added to the filtrate in an ice bath, and the yellow precipitate was collected by filtration. The precipitate was dissolved in 150 mL of cold dimethylformamide (DMF), and then 2-hydroxy-4-(octyloxy)benzophenone (10.2 g, 32.7 mmol) in cold DMF (80 mL) was added dropwise to this solution. The mixture was stirred at 0−5 °C. Subsequently, 15.0 g of sodium acetate in 80 mL of deionized water was added dropwise carefully, and a red precipitate was produced. The mixture was further stirred at room temperature for 1 h. The crude product was purified by recrystallization from a mixture of ethanol and ethyl acetate (1:1, v/v). The target product **1** was then obtained as a orange crystal (12.1 g, 79%). Elemental analysis: C 78.63% (calcd 78.23%), H 6.96% (calcd 6.76%), N 5.45% (calcd 5.53%). ^{1}H NMR (DMSO-d_6): 7.70−7.80 (m, 2H, aromatic), 7.44−7.57 (m, 5H, aromatic), 7.12−7.41 (m, 8H, aromatic), 6.67 (s, 1H, aromatic), 4.25 (t, 2H, ArOCH_2−), 2.00 (m, 2H, −OCH$_2$CH_2−), 1.31−1.56 (m, 10H, −CH_2−), 0.89 (t, 3H, −CH$_2$CH_3).

1′-Octyloxy-4′-hexyloxy-5′-phenylmethaneone-(2-phenyl)azobenzene (2). 1 (11.1 g, 22.0 mmol) was dissolved in 150 mL of DMF. Anhydrous potassium carbonate (7.6 g, 55 mmol) and a catalytic amount of potassium iodide (3.0 mg) were added. The mixture was heated to 110 °C with stirring, and 1-chloro-6-hydroxyhexane (7.5 g, 55 mmol) was added dropwise to the reaction mixture; the mixture reacted 24 h at 110 °C. Then, the reaction mixture was cooled to room temperature and poured into 1 L of deionized water. The precipitated was collected by filtration and purified by silica gel chromatography with a petroleum ether/ethyl acetate (2:1, v/v) mixture as eluent to yield the final product (**2**) as a red solid (11.3 g, 84%). Elemental analysis: C 76.33% (calcd 76.09%), H 6.99% (calcd 6.76%), N 5.35% (calcd 5.22%). ^{1}H NMR (DMSO-d_6): 7.60−7.63 (m, 6H, aromatic), 7.40−7.50 (m, 6H, aromatic), 7.31 (m, 3H, aromatic), 6.91 (s, 1H, aromatic), 4.26 (t, 2H, ArOCH_2−), 3.96 (t, 2H, ArOCH_2−), 3.58 (t, 2H, −CH_2OH), 1.97 (t, 2H, −OCH$_2$CH_2−), 1.09−1.60 (m, 18H, −CH_2−), 0.89 (t, 3H, −CH$_2$CH_3).

1′-Octyloxy-4′-(6-methacryloxy)hexyloxy-5′-phenylmethaneone-(2-phenyl)azobenzene (AHMA). Triethylamine (2.7 g, 27 mmol) was added to a solution of compound **2** (10.9 g, 18.0 mmol) in 150 mL of dry tetrahydrofuran (THF). The solution was stirred in an ice bath, and methacryloyl chloride (2.6 mL, 27 mmol) in dry THF (10 mL) was added dropwise under an argon atmosphere; the

mixture was then stirred at room temperature overnight. The solution was filtered, and the solvent was removed in vacuum. The crude product was dissolved in chloroform and washed with deionized water three times and then dried with anhydrous magnesium sulfate overnight. Finally, the obtained crude product was purified by recrystallization from ethanol to give a yellow crystal (8.5 g, 70%). Elemental analysis: C 76.28% (calcd 76.53%), H 7.58% (calcd 7.47%), N 4.25% (calcd 4.15%). ^{1}H NMR (DMSO-d_6): 7.58−7.64 (m, 6H, aromatic), 7.38−7.51 (m, 6H, aromatic), 7.30−7.23 (m, 3H, aromatic), 6.91 (s, 1H, aromatic), 6.10 (s, 1H, CH_2═), 5.56 (s, 1H, CH_2═), 4.26 (t, 2H, ArOCH_2−), 4.01−4.07 (m, 4H, ArOCH_2− and −CH_2OCO), 1.94−1.98 (m, 5H, −OCH$_2$CH_2− and CH_3OCO), 1.09−1.60 (m, 18H, −CH_2−), 0.89 (t, 3H, −CH$_2$CH_3). The ^{1}H NMR spectrum of AHMA is shown in Figure 1.

RAFT Polymerization of AHMA. The following procedure was typical: A master batch of AHMA (4.00 g, 5.93 mmol), AIBN (9.7 mg, 0.059 mmol), and CPDN (48.2 mg, 0.178 mmol) was dissolved in 25.0 mL of anisole, and 3.00 mL aliquots were placed in each ampule. The contents were purged with argon for ∼20 min to eliminate the dissolved oxygen. Then, the ampules were flame-sealed and placed in an oil bath held by a thermostat at the desired temperature to polymerize. At timed intervals, the tube was cooled in ice water and then opened. The polymers (PAHMA) were purified by precipitating twice from THF to petrol ether and dried in a vacuum oven overnight at 50 °C. The conversion of polymerization was determined gravimetrically.

The macro-RAFT agent was prepared with the similar procedures above. A round-bottom flask with a stir bar was charged with AHMA (3.50 g, 5.19 mmol), AIBN (17.7 mg, 0.108 mmol), CPDN (86.9 mg, 0.320 mmol), and 25.0 mL of anisole. The contents were purged with argon for ∼40 min to eliminate oxygen in the reaction system. The flask was sealed under argon and put in an oil bath at 70 °C for 6 h. The polymer was obtained by precipitating into petrol ether, followed with filtration. It was further purified by precipitating twice from THF to petrol ether and dried in a vacuum oven overnight at 50 °C. The conversion of monomer was determined gravimetrically (yield: 64.7%; $M_{n(GPC)}$ = 6200 g/mol and PDI = 1.20).

Chain Extension with PAHMA as a Macro-RAFT Agent. The RAFT block copolymerizations of MMA and St were carried out with the same procedure of RAFT polymerization of AHMA, except that CPDN was substituted by PAHMA obtained from the RAFT polymerization of AHMA.

Preparation of the Polymer Film. A polymer solution was obtained by solving the homopolymer (PAHMA) in THF with concentration of 0.1 g/mL. Thin film sample of homopolymer was prepared by spin-coating about 50 μL of the polymer solution onto clean glass slide at 1500 rpm. The thickness of the film was controlled to be about 1.0 μm. After dried under vacuum for 24 h to drive off residual solvent, the film was stored in a desiccator for further study.

Results and Discussion

RAFT Polymerization of AHMA. The RAFT polymerization of AHMA was carried out using CPDN as the RAFT agent and AIBN as the initiator in anisole solution. The effect of the polymerization temperature on the RAFT polymerization of AHMA was investigated, and the results are presented in Figures 3 and 4. As shown in Figure 3, the corresponding plots of ln([M]$_0$/[M]) vs the polymerization time were linear at 60 and 70 °C, respectively, which indicated that the propagating radical concentrations were almost constant during the processes of the polymerization. As shown in Figure 3, the polymerization rate of AHMA at 70 °C was faster than that at 60 °C, which could be attributed to the decomposition rate of AIBN, and the rates of propagation, addition, and fragmentation of the RAFT intermediates were all increased at higher temperature. There was an obvious inhibition period lasting up to 5 h at 60 °C.

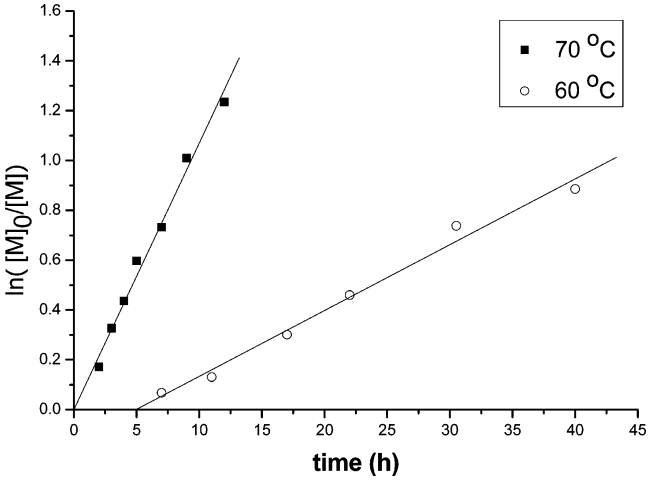

Figure 3. Relationships between ln([M]$_0$/[M]) and the polymerization time for the reversible addition−fragmentation chain transfer (RAFT) polymerization of AHMA in anisole at different temperatures. [AHMA]$_0$/[AIBN]$_0$/[CPDN]$_0$ = 100/1/3. AIBN = 2,2′-Azobis(isobutyronitrile); CPDN = 2-cyanoprop-2-yl-1-dithionaphthalate; AHMA = 1′-octyloxy-4′-(6-methacryloxy)hexyloxy-5′-phenylmethaneone-(2-phenyl)azobenzene.

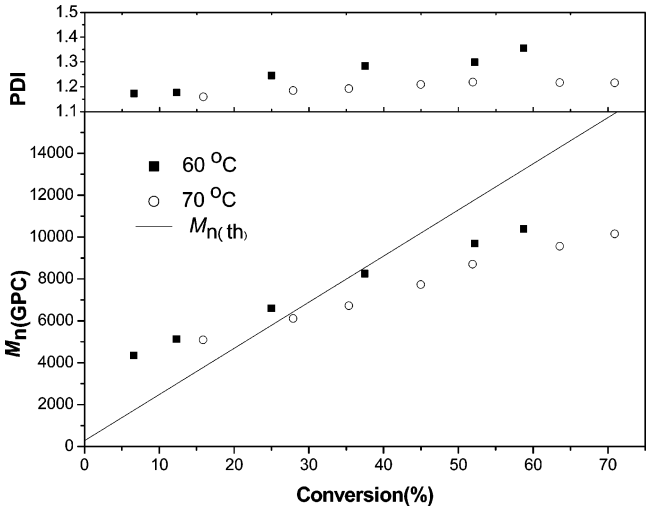

Figure 4. Evolution of $M_{n(GPC)}$ and PDI with monomer conversion for the reversible addition−fragmentation chain transfer (RAFT) polymerization of AHMA in anisole solution at different temperatures. Polymerization conditions are the same as in Figure 3. $M_{n(GPC)}$ = number-average molecular weight determined by gel permeation chromatograph; PDI = polydispersity index value; AHMA = 1′-octyloxy-4′-(6-methacryloxy)hexyloxy-5′-phenylmethaneone-(2-phenyl)azobenzene.

The inhibition period observed in the RAFT polymerization may be related to the slow reinitiation of the initiating and leaving group radicals during the period of consumption of the initial RAFT agent.[28,44,45]

Figure 4 shows the dependence of the $M_{n(GPC)}$s and PDIs on the monomer conversions. The $M_{n(GPC)}$s increased linearly with increasing monomer conversion, which was consistent with the polymerization proceeding in a controlled fashion. However, the $M_{n(GPC)}$s were slightly higher than the theoretical values in the early stage of the polymerization and lower than the theoretical values at relatively high conversions. The theoretical molecular weight ($M_{n(th)}$) was calculated as follows:

$$M_{n(th)} = ([\mathrm{AHMA}]_0/[\mathrm{CPDN}]_0) \times \mathrm{MW}_{\mathrm{AHMA}} \times \text{conversion} + \mathrm{MW}_{\mathrm{CPDN}}$$

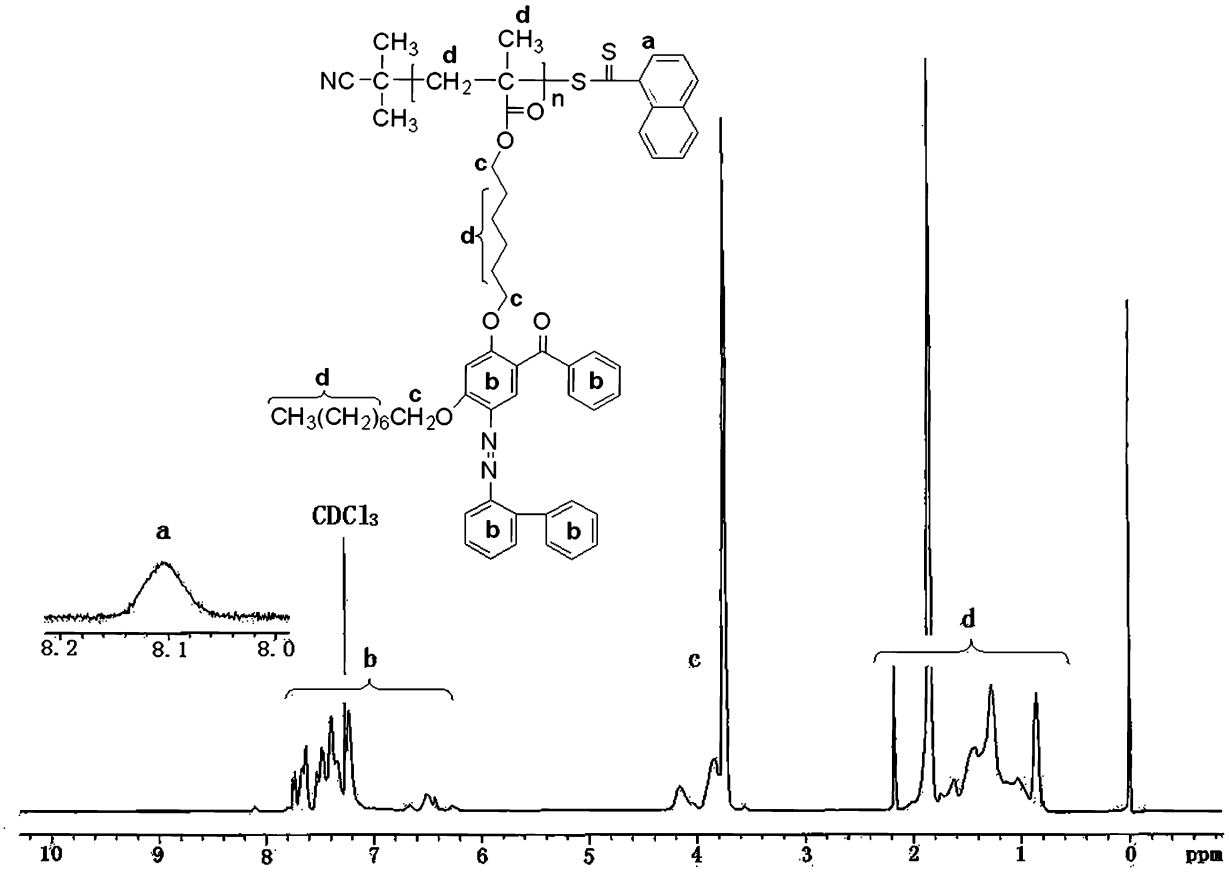

Figure 5. ^{1}H NMR spectrum of PAHMA in $CDCl_3$ solvent. ($M_{n(GPC)}$ = 5100 g/mol, PDI = 1.16). PAHMA = poly{1′-octyloxy-4′-(6-methacryloxy)-hexyloxy-5′-phenylmethaneone-(2-phenyl)azobenzene}.

where $[AHMA]_0$ and $[CPDN]_0$ are the initial concentration of AHMA and CPDN, respectively, and MW_{AHMA} and MW_{CPDN} are the molecular weight of AHMA and CPDN, respectively. At the beginning of the polymerization, some positive deviation of $M_{n(GPC)}$s from the theoretical values ($M_{n(th)}$s) may be due to the incomplete usage of RAFT agent. And at high monomer conversions, some negative deviation may be due to some side reactions of the initiator or initiator-derived radicals with the RAFT agent.[27,46] On the other hand, the GPC standard calibration samples of PMMA may be an other cause of some deviations from the theoretical values. The PDIs of the polymers were relatively low up to high conversions in all cases (PDI ≤ 1.37).

End-Group Analysis. Figure 4 shows the ^{1}H NMR spectrum of the PAHMA. The characteristic signals corresponding to the phenyl protons of the azobenzene group were observed from 6.20 to 7.85 ppm. The peaks at 8.14 ppm (a) corresponded to partial of the aromatic protons (a) in CPDN units, which proved that the RAFT agent was attached on the end of the polymer chain. The other characteristic signals of the aromatic protons in CPDN units were overlapped by the signals of phenyl protons of the polymer. The singals at 3.79 ppm should be assigned to the methylene group of $-CH_2-O-$ in the side chain. The peaks from 0.90 to 2.20 ppm were attributed to other methylene group and methyl groups.

Preparation of Block Copolymers. According to the RAFT mechanism, the obtained PAHMA could be used as a macro-RAFT agent to prepare different well-defined block copolymers. In this work, MMA and St were used as the monomers of chain extension, respectively. The block copolymerizations of MMA and St were carried out in anisole using PAHMA as the macro-RAFT agent and AIBN as the initiator at 70 °C. As shown in Figure 6, both kinetic plots were first-order until 86.6% conversion of MMA and 39.5% conversion of St, respectively. In the case of St, the polymerization rate decreased significantly when conversion was higher than 40%. A similar phenomenon was also observed in reference using macro-RAFT agent to polymerize other monomer.[39] Figure 7 shows that the corresponding $M_{n(GPC)}$s increased linearly with increasing monomer conversions. The PDIs of the two diblock copolymers of PAHMA-*b*-PMMA and PAHMA-*b*-PS were less than 1.47 and 1.38, respectively, which were relatively higher than that of the macro-RAFT agent (PDI = 1.20). This was contributed to the combination effects of homopolymerization of second monomer and a portion of dead chains existed in the macro-RAFT agent (shown as shoulders at low molecular weights in the GPC curves, Figures 8 and 9).

The successful RAFT block copolymerization of MMA and St using PAHMA as a macro-RAFT agent showed "living"/controlled way, and these results implied that most of the PAHMA chains were still "living". As the result, RAFT polymerization method may be served as an effective method to prepare azo block copolymers from an azo macro-RAFT agent.

Photoisomerization. The UV−vis absorption spectrum of the azo polymer will change when the configuration changes from trans to cis upon irradiation.[47] To investigate this character of the PAHMA, the UV−vis spectra of PAHMA in chloroform were characterized. As shown in Figure 10, the polymer exhibited two strong absorption peaks. The first peak at 245 nm appearing in the shorter wavelength region corresponded to the absorption of the phenyl moiety, and the second peak at

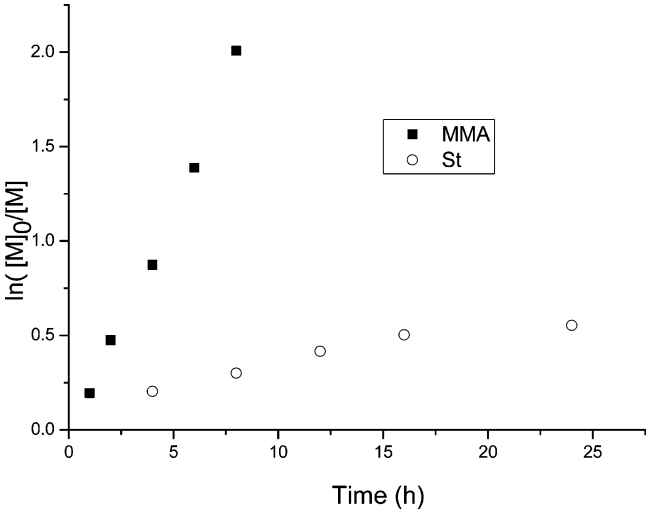

Figure 6. Relationships between $\ln([M]_0/[M])$ and the polymerization time for the reversible addition−fragmentation chain transfer (RAFT) block copolymerization of MMA and St in anisole with AIBN as initiator using PAHMA as the macro-RAFT agent. Polymerization conditions: $[MMA]_0/[AIBN]_0/[PAHMA]_0 = 1000/1/3$, MMA/anisole (v/v) = 1/1, 70 °C and $[St]_0/[AIBN]_0/[PAHMA]_0 = 800/1/3$, St/anisole (v/v) = 1/1, 70 °C. MMA = methyl methacrylate; St = styrene; AIBN = 2,2′-azobis(isobutyronitrile); PAHMA = poly{1′-octyloxy-4′-(6-methacryloxy)hexyloxy-5′-phenylmethaneone-(2-phenyl)azobenzene}; RAFT = reversible addition−fragmentation chain transfer; $M_{n(GPC)}$ = number-average molecular weight determined by gel permeation chromatograph; PDI = polydispersity index value.

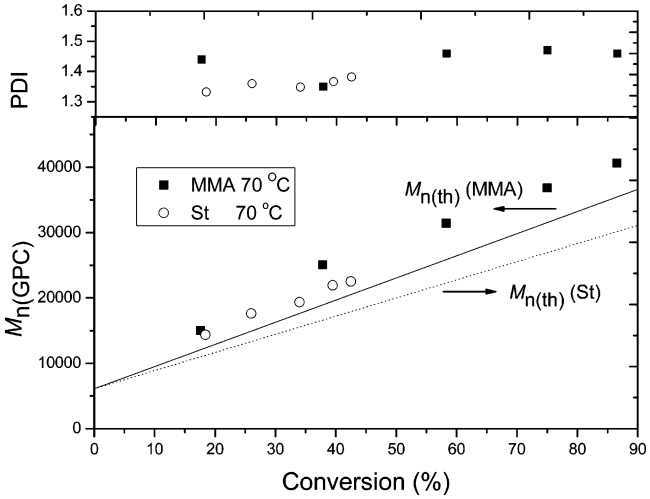

Figure 7. Evolution of $M_{n(GPC)}$ and PDI with monomer conversion for the reversible addition−fragmentation chain transfer (RAFT) block copolymerization of MMA and St with AIBN as initiator in anisole using PAHMA as a macro-RAFT agent. Polymerization conditions are same as in Figure 6. $M_{n(GPC)}$ = number-average molecular weight determined by gel permeation chromatograph; PDI = polydispersity index value; MMA = methyl methacrylate; St = styrene; AIBN = 2,2′-azobis(isobutyronitrile); PAHMA = poly{1′-octyloxy-4′-(6-methacryloxy)hexyloxy-5′-phenylmethaneone-(2-phenyl)azobenzene}.

about 375 nm was attributed to the absorption of the azo moiety in the side chains of polymer; the trans form of the azo chromophore in PAHMA changed to the cis form after being irradiated with 364 nm UV light. The top curve (a) corresponded to the spectrum before irradiation; therefore, all the azo chromophores were almost in the trans state. Upon irradiation at 364 nm, the absorbance at 460 nm corresponding to the $n-\pi^*$ transition (cis state) increased with the irradiation time, while the absorbance at 375 nm corresponding to the $\pi-\pi^*$ transition (trans state) decreased with irradiation time.[48] The photostationary state was obtained after irradiation for 240 s photoisomerization. The proportion of isomerization at the photostationary state was estimated with the equation $100(A_0 - A_t)/A_0$ (%), where A_0 and A_t are the absorptions at the maximum wavelength of 375 nm before and after irradiation, respectively. The cis content was about 34% in the photostationary state, and the low cis content may be due to the relatively slow thermal cis−trans isomerization rate.

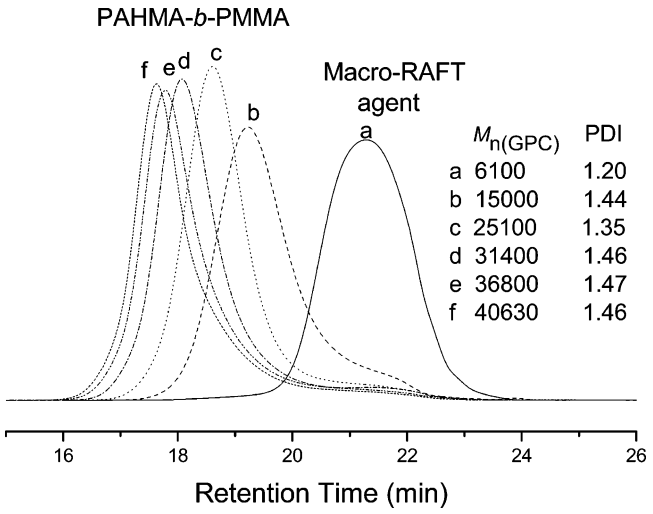

Figure 8. GPC trace for PAHMA-*b*-PMMA for chain extension using PAHMA as macro-RAFT agent. PAHMA = poly{1′-octyloxy-4′-(6-methacryloxy)hexyloxy-5′-phenylmethaneone-(2-phenyl)azobenzene}; MMA = poly(methyl methacrylate); RAFT = reverse addition−fragmentation chain transfer.

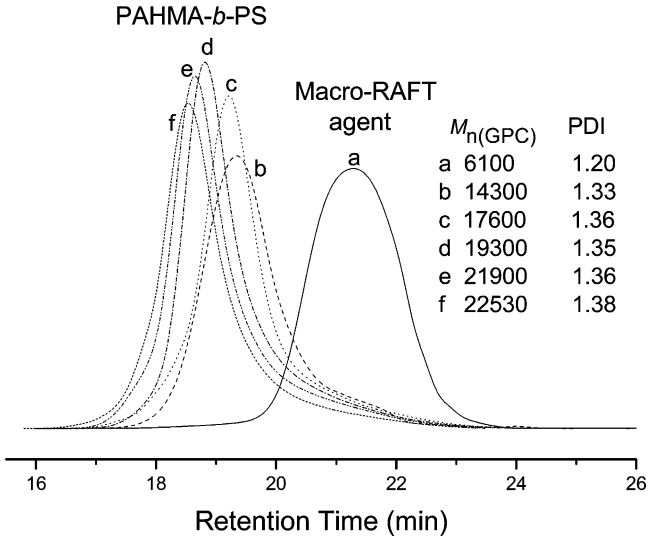

Figure 9. GPC trace for PAHMA-*b*-PS for chain extension using PAHMA as macro-RAFT agent. PAHMA = poly{1′-octyloxy-4′-(6-methacryloxy)hexyloxy-5′-phenylmethaneone-(2-phenyl)azobenzene}; St = poly(styrene); RAFT = reversible addition−fragmentation chain transfer.

Photoinduced Birefringence. With the presence of substituted azobenzene chromophores, the PAHMA was highly sensitive to the polarization of the actinic light and become anisotropic when irradiated with a linearly polarized light. This was a consequence of the polarization sensitive rodlike *trans*-azobenzene chromophores.[49] After irradiation with a linearly polarized light, the azobenzene groups undergo a trans−cis photoisomerization followed by an angular reorientation of the chromophore in a perpendicular direction with respect to the incident polarization. A typical writing−erasing curve of optically induced and subsequently eliminated birefringence for PAHMA sample at room temperature is presented in Figure

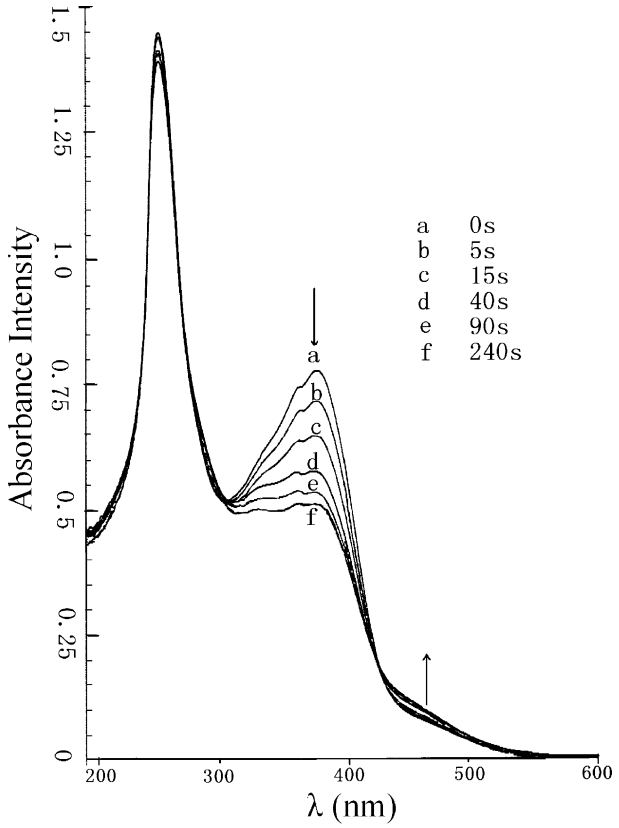

Figure 10. Changes in the UV−vis absorption spectra of PAHMA ($M_{n(GPC)}$ = 10 200 g/mol, PDI = 1.22) during the irradiation (with 364 nm UV light) in chloroform. The irradiation times are (a) 0, (b) 5, (c) 15, (d) 40, (e) 90, and (f) 240 s. $[PAHMA]_0 = 3.4 \times 10^{-5}$ g/mL in chloroform). PAHMA = poly{1′-octyloxy-4′-(6-methacryloxy)hexyloxy-5′-phenylmethaneone-(2-phenyl)azobenzene}; $M_{n(GPC)}$ = number-average molecular weight determined by gel permeation chromatograph; PDI = polydispersity index value.

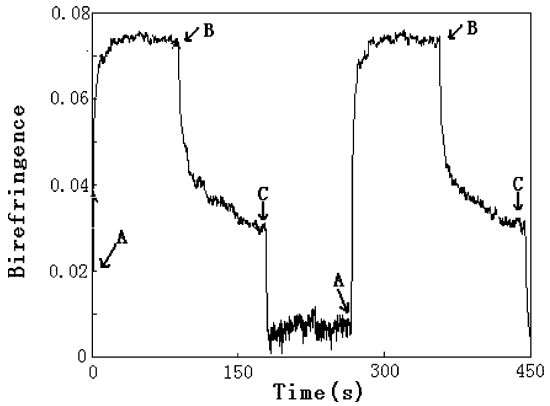

Figure 11. Typical behavior of the photoinduced birefringence for PAHMA at room temperature: A = writing laser is turned on, B = writing laser is turned off, and C = erasing laser is turned on. The PAHMA polymer used is the same as present in Figure 10.

11. Before irradiation, no optical anisotropy was observed because of the homogeneously random alignment of the azobenzene chromophores. The birefringence was induced immediately under irradiation with a linearly polarized UV laser as the result of the alignment of the azo chromophores perpendicular to the laser polarization occurred on account of the trans−cis−trans isomerization of azo moieties. At point A, the linearly polarized writing laser beam at 413.1 nm light (20 mW/cm^2) was engaged, and the photoinduced birefringence was induced quickly and stabilized after about 35 s. The maximum values of the photoinduced birefringence for sample reached about 0.075. At point B, when the excitation beam was turned off, about 60% of the photoinduced birefringence was lost quickly and stabilized at about 0.03. This change in relaxation level must be attributed mainly to motion arising from heat dissipation. As PAHMA is not the donor−acceptor substituted azo polymer, the thermal cis−trans isomerization rate is much slower. The cis−trans isomerization plays a less significant impact on the decrease of birefringence.[50] Similar to amorphous azobenzene polymers, the remaining photoinduced anisotropy can be erased when a circularly polarized excitation beam was turned on at point C. The effect of circularly polarized light was to randomize back the orientation of the azobenzene groups. The cycle between the birefringence induction, relaxation, and erasure can be repeated in the same manner with the same level of birefringence at the same rate. The behavior was very similar to that of the donor−acceptor substituted azobenzene polymers.

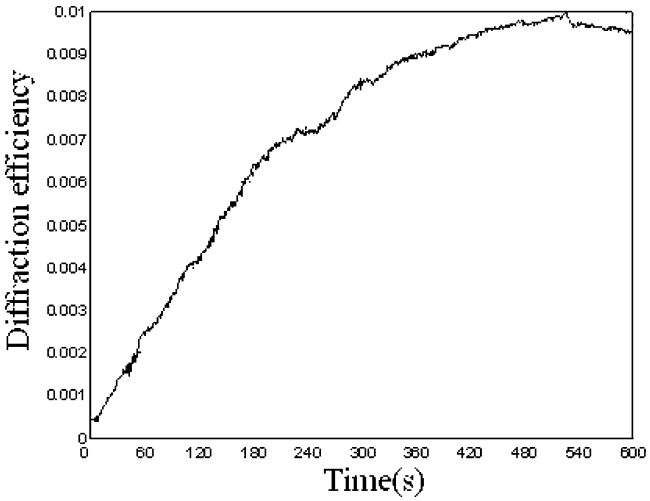

Figure 12. Diffraction efficiency of the surface relief gratings inscribed on the PAHMA film as a function of irradiation time. The PAHMA polymer used is the same as present in Figure 10.

Photoinduced Surface Relief Gratings. For optical storage properties, creation of local holographic gratings is very important, and it is customary to report the diffraction efficiencies achieved on various materials.[50] SRGs can easily be inscribed by a single-step all-optical process, in contrast to other methods such as chemical etching or photoresist processing. The photofabrication of the SRGs was performed on spin-coated thin films of the PAHMA with a thickness of about 1 μm. Using suitable wave plates, these two beams which were orthogonally polarized will be two p-polarized and used to produce the interference pattern on the polymer films. Relatively low light intensity (120 mW/cm^2) was used to write the gratings in order to avoid the sample damage and the other possible side effects caused by high-intensity laser irradiation.

The rates of gratings formation can be probed by measuring the first-order diffraction efficiency of the SRGs during the gratings inscription process.[51] After 500 s irradiation at room temperature, SRGs were saturated. A plot of the diffraction efficiency with respect to the exposure time is shown in Figure 12. Diffraction efficiency of about 1% was obtained in 500 s. The resultant surface peak-to-trough modulation has been characterized by AFM. The results are presented in Figures 13. A regularly spaced sinusoidal pattern can be seen in the plane and three-dimensional images. The spacing of the gratings was measured to be 0.6 μm, and the depth was 6 nm. The depth can be adjusted by the irradiation energy. The spatial period

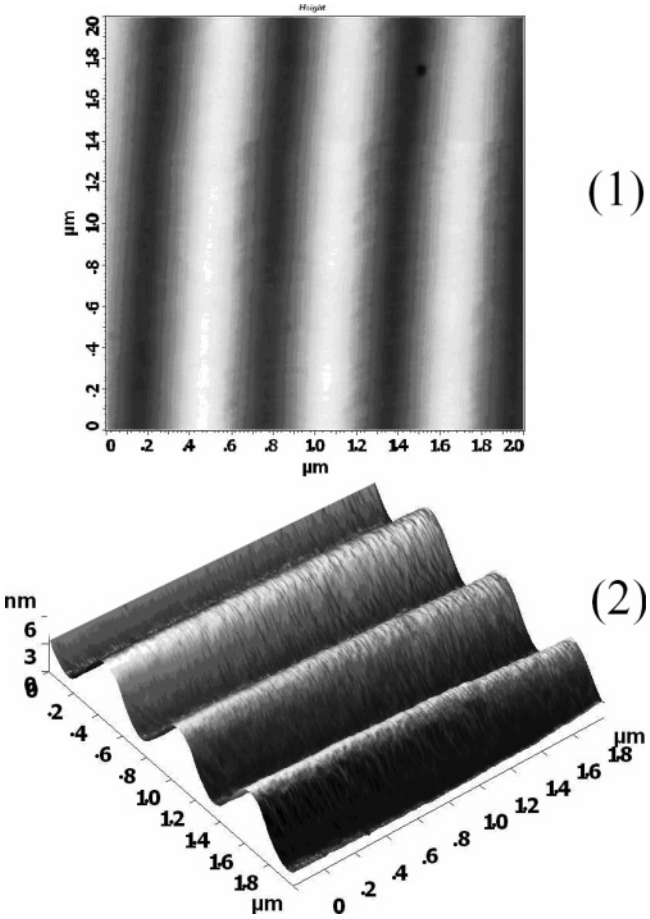

Figure 13. The (1) plane and (2) three-dimensional views of the photoinduced surface relief gratings.

depends on both the wavelength λ of the writing beam and the angle θ between the two interfering beams. Compared with other donor−acceptor substituted photoinduced azo SRGs,[11,40,41] the diffraction efficiency was relatively low and similar to that of no donor−acceptor substituted azobenzene polymers.[50]

Conclusions

The RAFT polymerization of azo monomer, AHMA, was successfully carried out using CPDN as RAFT agent and AIBN as the initiator in anisole. The polymerization showed typical "living"/controlled free radical polymerization behaviors. Most of the PAHMA macro-RAFT agents were still "living", and PAHMA-*b*-PMMA and PAHMA-*b*-PS diblock copolymers were also successfully synthesized using PAHMA as the macro-RAFT agent. The PAHMA in chloroform solution exhibited the photoisomeric behavior of the polymers with azobenzene group. On irradiation with a linearly polarized laser beam, birefringence was induced in the azo polymer film to the level of 0.075. The surface relief gratings with 1% diffraction efficiency formed on the polymer film surface were obtained with 500 s of irradiation at recording beam intensity of 120 mW/cm^2 at modest intensities.

Acknowledgment. The financial support of this work by the National Nature Science Foundation of China (No. 20574050), the Science and Technology Development Planning of Jiangsu Province (No. BG2004018) and Suzhou City (Nos. SG0413 and SSZ0419), the Nature Science Key Basic Research of Jiangsu Province for Higher Education (No. 05KJA15008), and the Specialized Research Fund for the Doctoral Program of Higher Education (No. 20040285010) is gratefully acknowledged.

References and Notes

(1) Ichimura, K. *Chem. Rev.* **2000**, *100*, 1847−1873.
(2) Natansohn, A.; Rochon, P. *Chem. Rev.* **2002**, *102*, 4139−4175.
(3) Pedersen, T. G.; Johansen, P. M.; Pedersen, H. C. *J. Opt. A: Pure Appl. Opt.* **2000**, *2*, 272−278.
(4) Wu, Y.; Kanazawa, A.; Shiono, T.; Ikeda, T.; Zhang, Q. *Polymer* **1999**, *40*, 4787−4793.
(5) Hafiz, H. R.; Nakanishi, F. *Nanotechnology* **2003**, *14*, 649−654.
(6) Barrett, C.; Rochon, P.; Natansohn, A. *J. Chem. Phys.* **1998**, *109*, 1505−1516.
(7) Kim, D. Y.; Tripathy, S.; Li, L.; Kumar, J. *Appl. Phys. Lett.* **1995**, *66*, 1166−1168.
(8) Todorov, T.; Tomova, N.; Nikolova, L. *Opt. Commun.* **1983**, *47*, 123−126.
(9) Todorov, T.; Nikolova, L.; Tomova, N. *Appl. Opt.* **1984**, *23*, 4309−4312.
(10) Natansohn, A.; Xie, S.; Rochon, P. *Macromolecules* **1992**, *25*, 5531−5532.
(11) Ho, M. S.; Barrett, C.; Paterson, J.; Esteghamatian, M.; Natansohn, A.; Rochon, P. *Macromolecules* **1996**, *29*, 4613−4618.
(12) Wu, Y.; Natansohn, A.; Rochon, P. *Macromolecules* **2004**, *37*, 6090−6095.
(13) Andruzzi, L.; Hvilsted, S.; Ramanujam, P. S. *Macromolecules* **1999**, *32*, 448−454.
(14) Barrett, C.; Natansohn, A.; Rochon, P. *J. Phys. Chem.* **1996**, *100*, 8836−8842.
(15) Jiang, X. L.; Li, L.; Kumar, J.; Kim, D. Y.; Tripathy, S. K. *Appl. Phys. Lett.* **1998**, *72*, 2502−2504.
(16) Viswanathan, N. K.; Balasubramanian, S.; Li, L.; Kumar, J.; Tripathy, S. K. *J. Phys. Chem. B* **1998**, *102*, 6064−6070.
(17) Kumar, J.; Li, L.; Jiang, X. L.; Kim, D. Y.; Lee, T. S.; Tripathy, S. *Appl. Phys. Lett.* **1998**, *72*, 2096−2098.
(18) Pedersen, T. G.; Johansen, P. M.; Holme, N. C. R.; Ramanujam, P. S.; Hvilsted, S. *Phys. Rev. Lett.* **1998**, *80*, 89−92.
(19) Kim, D. Y.; Li, L.; Jiang, X. L.; Shivshankar, V.; Kumar, J.; Tripathy, S. K. *Macromolecules* **1995**, *28*, 8835−8839.
(20) Altomare, A.; Ciardelli, F.; Tirelli, N.; Solaro, R. *Macromolecules* **1997**, *30*, 1298−1303.
(21) Yoshida, T.; Kanaoka, S.; Aoshima, S. *J. Polym. Sci.., Part A: Polym. Chem.* **2005**, *43*, 4292−4297.
(22) Kato, M.; Kamigaito, M.; Sawamoto, M.; Higashimura, T. *Macromolecules* **1995**, *28*, 1721−1723.
(23) Wang, J. S.; Matyjaszewski, K. *Macromolecules* **1995**, *28*, 7901−7910.
(24) Matyjaszewski, K.; Xia, J. H. *Chem. Rev.* **2001**, *101*, 2921−2990.
(25) Chiefari, J.; Chong, Y. K.; Ercole, F.; Kristina, J.; Jeffery, J.; Le, T. P. T.; Mayadunne, R. T. A.; Meijs, G. F.; Moad, C. L.; Moad, G.; Rizzardo, E.; Thang, S. H. *Macromolecules* **1998**, *31*, 5559−5562.
(26) Le, T. P.; Moad, G.; Rizzardo, E.; Thang, S. H. PCT Int. Pat. Appl. WO 9801478 Al, 1998.
(27) (a) Moad, G.; Rizzardo, E.; Thang, S. H. *Aust. J. Chem.* **2005**, *58*, 379−410. (b) Moad, G.; Rizzardo, E.; Thang, S. H. *Aust. J. Chem.* **2006**, *59*, 669−692. (c) Favier, A.; Charreyre, M. T. *Macromol. Rapid Commun.* **2006**, *27*, 653−692.
(28) Perrier, S.; Takolpuckdee, P. *J. Polym. Sci., Part A: Polym. Chem.* **2005**, *43*, 5347−5393.
(29) Tian, Y. Q.; Watanabe, K.; Kong, X. X.; Abe, J.; Iyoda, T. *Macromolecules* **2002**, *35*, 3739−3747.
(30) He, X. H.; Yan, D. Y. *Macromol. Rapid Commun.* **2004**, *25*, 949−953.
(31) Cui, L.; Zhao, Y.; Yavrian, A.; Galstian, T. *Macromolecules* **2003**, *36*, 8246−8252.
(32) Cui, L.; Tong, X.; Yan, X. H.; Liu, G. J.; Zhao, Y. *Macromolecules* **2004**, *37*, 7097−7104.
(33) Sin, S. L.; Gan, L. H.; Hu, X.; Tam, K. C.; Gan, Y. Y. *Macromolecules* **2005**, *38*, 3943−3948.
(34) Han, Y. K.; Dufour, B.; Wu, W.; Kowalewski, T.; Matyjaszewski, K. *Macromolecules* **2004**, *37*, 9355−9365.
(35) Barner-Kowollik, C.; Davis, T. P.; Heuts, J. P. A.; Stenzel, M. H.; Vana, P.; Whittaker, M. *J. Polym. Sci., Part A: Polym. Chem.* **2003**, *41*, 365−375.
(36) Zhang, L.; Yu, K.; Eisenberg, A. *Science* **1996**, *272*, 1777−1779.
(37) Chong, Y. K.; Le, T. P. T.; Moad, G.; Rizzardo, E.; Thang, S. H. *Macromolecules* **1999**, *32*, 2071−2074.
(38) Mayadunne, R. T. A.; Rizzardo, E.; Chiefari, J.; Krstina, J.; Moad, G.; Postma, A.; Thang, S. H. *Macromolecules* **2000**, *33*, 243−245.

(39) Albertin, L.; Stenzel, M. H.; Barner-Kowollik, C.; Foster, L. J. R.; Davis, T. P. *Macromolecules* **2005**, *38*, 9075−9084.
(40) Darracq, B.; Chaput, F.; Lahlil, K.; Levy, Y.; Boilot, J. P. *Adv. Mater.* **1998**, *10*, 1133−1136.
(41) Che, P. C.; He, Y. N.; Wang, X. G. *Macromolecules* **2005**, *38*, 8657−8663.
(42) Takase, H.; Natansohn, A.; Rochon, P. *Polymer* **2003**, *44*, 7345−7351.
(43) Zhu, J.; Zhu, X. L.; Cheng, Z. P.; Liu, F. *Polymer* **2002**, *43*, 7037−7042.
(44) McLeary, J. B.; Calitz, F. M.; McKenzie, J. M.; Tonge, M. P.; Sanderson, R. D.; Klumperman, B. *Macromolecules* **2004**, *37*, 2383−2394.
(45) McLeary, J. B.; Calitz, F. M.; McKenzie, J. M.; Tonge, M. P.; Sanderson, R. D.; Klumperman, B. *Macromolecules* **2005**, *38*, 3151−3161.
(46) Chong, Y. K.; Krstina, J.; Le, T. P. T.; Moad, G.; Rizzardo, E.; Thang, S. H. *Macromolecules* **2003**, *36*, 2256−2272.
(47) Zimmerman, G.; Chow, L.; Paik, U. *J. Am. Chem. Soc.* **1958**, *80*, 3528−3531.
(48) Mochizuki, H.; Nabeshima, Y.; Kitsunai, T.; Kanazawa, A.; Shiono, T.; Ikeda, T.; Hiyama, T.; Maruyama, T.; Yamamoto, T.; Koide, N. *J. Mater. Chem.* **1999**, *9*, 2215−2219.
(49) Iftime, G.; Lagugne, F.; Labarthet, F. L.; Natansohn, A.; Rochon, P.; Murti, K. *Chem. Mater.* **2002**, *14*, 168−174.
(50) Natansohn, A.; Rochon, P.; Ho, M. S.; Barrettt, C. *Macromolecules* **1995**, *28*, 4179−4183.
(51) Rochon, P.; Batalla, E.; Natansohn, A. *Appl. Phys. Lett.* **1995**, *66*, 136−138.

MA070257I